CRYSTAL GROWTH & DESIGN
2008
VOL. 8, NO. 8
3073–3076

Controlled Growth and Phase Transition of Silver Nanowires with Dense Lengthwise Twins and Stacking Faults

Biao Wang, Guang Tao Fei,* Ye Zhou, Bing Wu, Xiaoguang Zhu, and Lide Zhang

Key Laboratory of Materials Physics and Anhui Key Laboratory of Nanomaterials and Nanostructures, Institute of Solid State Physics, Hefei Institutes of Physical Science, Chinese Academy of Sciences, Hefei 230031, P. R. China

Received February 26, 2008; Revised Manuscript Received May 21, 2008

ABSTRACT: Large-scale face-centered cubic (FCC)-Ag nanowires with dense (111) stacking faults and (111)/[112] growth twins were prepared by the electrodeposition in the holes of porous alumina template. The obtained twins and stacking faults in Ag nanowires are parallel to the axis of the nanowire and persist along the whole wire length. Importantly, novel 4H-Ag nanowires can form spontaneously after aging or heating this kind of FCC-Ag nanowire. This study contributes to the understanding of planar defect formation in the electrodeposition process and could be used to control the crystalline structure of Ag nanowires.

1. Introduction

Controlled growth of nanowires is an important research field and has attracted considerable attention recently.[1,2] Metallic nanowires are the most interesting materials for the exploration of the growth mechanisms. It is well-known that the physical properties of metallic nanowires strongly depend on their microstructures.[3,4] Stacking faults and growth twins, which are common microstructures in face-centered cubic (FCC) metals or alloys, are frequently observed in nanomaterials.[5,6] As the major planar defects, they can act as obstacles to the movement of dislocations; therefore, they have important effects on the deformation behavior of nanomaterials.[7] Recently, Lu et al.[5] synthesized pure bulk copper samples with a high density of growth twins. They found that the obtained samples show a tensile strength about 10 times higher than that of conventional coarse-grained copper, while retaining an electrical conductivity comparable to that of pure copper. However, in contrast to the extensively studied morphological changes in shape and size, the control of the microstructure inside nanowires has rarely been reported. Therefore, it is interesting to study the growth twins and stacking faults in metallic nanowires, especially to control the microstructure.

Among all the metals, silver is particularly important as it possesses the highest electrical conductivity and promising potential applications in many fields, such as catalysts and electronic nanodevices.[8–11] The template method is a versatile technique for the fabrication of nanowires with uniform diameters ranging from several to hundreds of nanometers in large area, and the properties of the nanowires can be tailored by adjusting the deposition conditions.[12–14] Ag nanowire obtained by the template method at high overpotential is polycrystalline because the growth of Ag nanowire follows a three-dimensional (3D) nucleation mechanism at high overpotential.[15] Many groups reported that dense growth twins and stacking faults could be found in these polycrystalline Ag nanowires.[15,16] Recently, Uchihashi et al.[17] reported that Ag film grown on an atomic-scale geometrical template through low-temperature deposition has stripe structures, and this film is in FCC structure with periodic insertion of stacking faults. Similarly, it is well-known that epitaxial films can also be deposited on the substrates at low overpotential.[18] To our best knowledge, no research has paid attention to the controlled growth of twins and stacking faults in epitaxial metallic nanowires. In this study, we take Ag nanowires as an example to control the growth of twins and stacking faults in electrodeposition. First, we prepared polycrystalline Ag nanocrystals with dense planar defects at high overpotential. Subsequently, we deposited epitaxial Ag nanowires at low overpotential on these polycrystalline Ag nanocrystals. By this two-step deposition process, Ag nanowires with dense lengthwise (111) stacking faults and (111)/[112] growth twins (GS-Ag) were successfully fabricated. More importantly, we found that 4H-Ag phase formed spontaneously after these GS-Ag nanowires were aged or annealed.

2. Experimental Section

The porous anodic alumina membrane (AAM) templates were prepared by a two-step anodization process proposed by Masuda et al.[19–21] Prior to anodization, high purity aluminum foils (99.999%) were degreased in acetone. Subsequently, the foils were annealed in a vacuum of 10^{-5} Pa at 500 °C for 5 h to remove the mechanical stress. Anodization was first carried out in 0.3 M $H_2C_2O_4$ at 15 °C for 4 h. After removing of the alumina layer in a mixture of 6 wt % H_3PO_4 and 1.5 wt% $H_2Cr_2O_4$, the aluminum foils were oxidized again for 20 h at the same conditions mentioned above. The remaining aluminum was removed by a saturated $SnCl_4$ solution. The alumina barrier layer was dissolved in 5 wt % H_3PO_4 solution at 30 °C. The pore of the AAM can be enlarged by immersing the AAM into 5 wt % H_3PO_4 solution and the pore size can be controlled by the etching time. The pore diameter of AAM used here is about 40 nm, the thickness of the AAM is 50 μm, and the pore density is about 2.3×10^{10} cm^{-2}.

A layer of Au film serving as the working electrode was sputtered onto one side of the AAM. The electrodeposition process was carried out in a common two-electrode electrochemical cell at 0 °C. The electrolyte consisted of 90 g L^{-1} $AgNO_3$, 30 g L^{-1} H_3BO_4, 7 g L^{-1} $C_4H_6O_6$ and 30 g L^{-1} $NaNO_3$; the initial pH value was adjusted to 3 by adding appropriate amounts of saturated Na_2CO_3 solution.

Samples collected at different steps were characterized by an X-ray diffractometer (XRD) (Philips X'Pert) with Cu Kα_1 radiation (λ = 1.54056 Å), a Sirion 200 field-emission scanning electron microscope (SEM) operated at 5 kV, and a JEM-2010 high-resolution electron microscope (HR-TEM). For XRD measurements, the sputtered Au and overfilled Ag film on the surface of the AAM template were mechanically polished away. For SEM observations, the AAM was dissolved with 0.5 M NaOH solution, and then carefully rinsed with deionized water for several times. For TEM observations, the AAM was completely dissolved with 0.5 M NaOH solution and then rinsed with absolute ethanol.

* Corresponding author. E-mail: gtfei@issp.ac.cn.

10.1021/cg800212z CCC: $40.75
Published on Web 07/17/2008

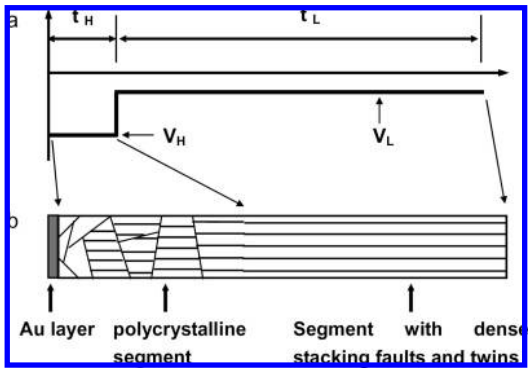

Figure 1. Schematic illustration of the synthesis of Ag nanowires: (a) the high and following low potential used in the two-step electrodeposition process; (b) illustration of the formation of Ag nanowire consisting of dense growth twins and stacking faults.

3. Results and Discussion

Figure 1 illustrates the electrodeposition process of this kind of GS-Ag nanowire. A high deposition voltage V_H of −0.95 V followed by a low deposition voltage V_L of −0.7 V was employed to prepare GS-Ag nanowires. The deposition current densities of polycrystalline segment and epitaxial segments are about 2 mA cm^{-2} and 0.2 mA cm^{-2}, respectively.

Figure 2a shows a SEM image of the freestanding GS-Ag nanowires, the AAM was completely dissolved by chemical etching. It is obvious that the nanowires have a high aspect ratio and the diameter is around 40 nm. Figure 2b shows a TEM image of a random selected silver nanowire. There is a junction existing in this nanowire, which is proven by the HRTEM image shown in Figure 2e. Selected area electron diffraction (SAED) indicates that the segment below the junction is polycrystalline (Figure 2c), and the segment above the junction contains a high density of (111) stacking faults and (111)/[112] type growth twins (Figure 2d). The presence of stacking faults and growth twins in Ag nanowire above the junction is further conformed by the HRTEM image shown in Figure 2f,g. The HRTEM image (Figure 2g) shows that the high-density interfaces divide the Ag nanowire into lamellar structures, the Ag lamellas are perfectly coherent and atomically sharp, and their thickness varies from 1 nm to about 3 nm. Importantly, the structure of the Ag nanowire does not change along the length of the whole nanowire above the junction, which is direct evidence of a 2D layer growth mechanism.

The electrodeposition is a complicated process and the structure of silver nanowires prepared by the template method is closely related to the deposition conditions. It has been reported that crystalline metallic nanowires will grow when the nucleus size exceeds the critical dimension Nc (cm). For 2D-like growth, Nc can be expressed as[15,22]

$$\mathrm{Nc} = bs\varepsilon^2/(ze\eta)^2 \quad (1)$$

where b (cmV^2/J^2), s (cm^2), ε (J/cm), z, and η (V) are a constant, the area occupied by one metallic atom on the surface of the nucleus, the edge energy, the effective electron number and the overpotential, respectively. According to the above expression, the lower overpotential η results in a larger Nc, which is more favorable for the growth of single-crystal nanowires. On the other hand, the Nc at high overpotential is smaller, which favors the 3D growth mode. Hence the Ag segment obtained at high deposition voltage of −0.95 V is polycrystalline. In general, the FCC-Ag nanowires deposited in the AAM pores always have

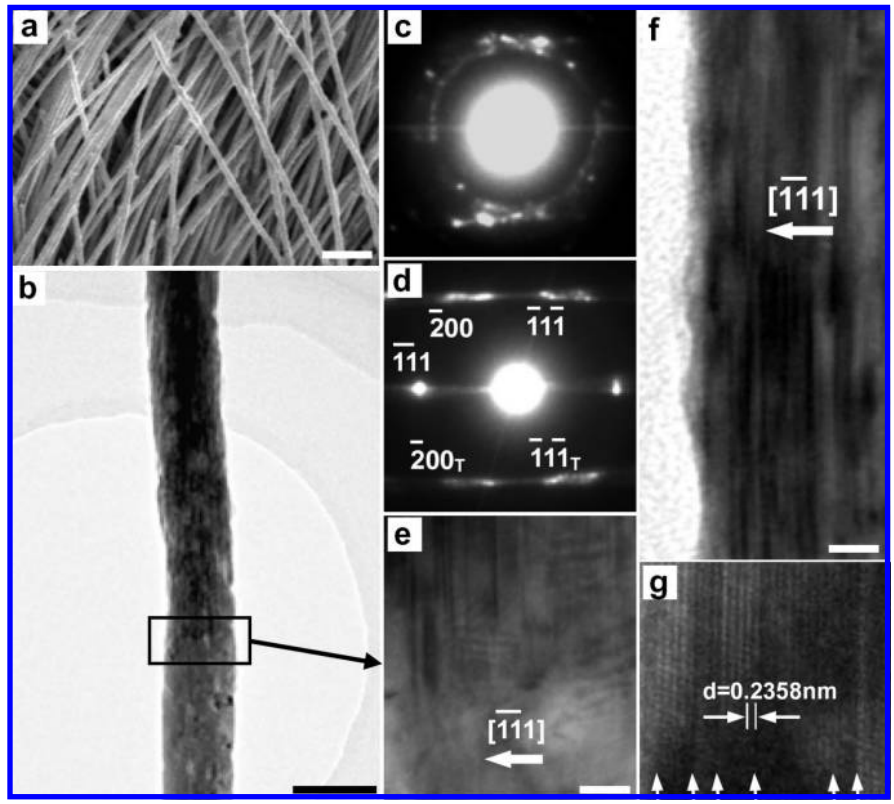

Figure 2. Ag nanowire structures: (a) SEM image of free-standing nanowires. Scale bars, 200 nm; (b) TEM image of a 40-nm-diameter nanowire. Scale bar, 50 nm; (c) electron pattern of the area below the junction; (d) electron pattern of the area above the junction; (e) HRTEM image of the boxed area of nanowire, Scale bar, 5 nm; (f) HRTEM image of the nanowire above the junction, Scale bar, 10 nm; (g) HRTEM image of the nanowire at high magnification, revealing the coherent stacking faults and growth twins planes (arrowhead).

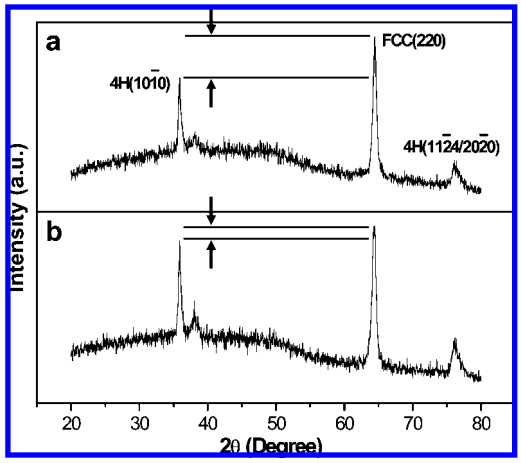

Figure 3. XRD patterns of Ag nanowire: (a) the GS-Ag nanowires after aging for 30 h; (b) the Ag nanowires after aging for 4 months. The peak located at $2\theta = 64.45°$ can be assigned to (220) planes of FCC-Ag; two peaks located at $2\theta = 35.94°$ and $2\theta = 76.12°$ can be assigned to (10$\bar{1}$0) and (11$\bar{2}$4) or (20$\bar{2}$0) planes of 4H-Ag.

a preferred orientation along the [220] direction.[22] Therefore, the adjacent Ag grains may share a common (110) plane in order to minimize the surface energy when the fine Ag grains nucleate and coalesce with each other during the high potential deposition process.[15] Furthermore, dense (111) stacking faults and (111)/[112] type growth twins would form in this oriented attachment process when a slight misorientation exists at the interfaces.[16] Based on the thermodynamic viewpoint, the excess energy of coherent interfaces is much smaller than that of incoherent grain boundaries. So stacking faults and growth twins with coherent interfaces are easily formed in order to reduce the total interfacial energy.[5]

In the low potential deposition process, epitaxial GS-Ag nanowires consisting of the same lengthwise planar defects would form spontaneously on polycrystalline Ag substrate which works as an atomic-scale geometrical template. Obviously, the formation of stacking faults and growth twins is due to the low energy of Ag stacking fault. Experimental and theoretical works showed that Ag has a low stacking fault energy (stacking fault energy per area is from 18 to 38 mJ m^{-2}).[23–25] This is smaller by an order of magnitude than that of other transition FCC metals. Therefore, GS-Ag nanowires consisting of dense lengthwise (111) stacking faults and (111)/[112] type growth twins would easily form during this electrodeposition process. The density of twins and stacking faults in nanowires are controlled by the deposition conditions. Our experimental observations show that when the current density at beginning is high or the pH value of the electrolyte is large or the deposition temperature is low, more twins and stacking faults are formed in the epitaxial Ag nanowires. We also found that when the deposition temperature is above 30 °C or the electrolyte pH is below 1, only the ordinary single-crystal FCC-Ag nanowires form and the planar defects in nanowires disappear.

Figure 3a shows the typical X-ray diffraction (XRD) pattern of GS-Ag sample deposited for 20 h and then placed at room temperature (about 20 °C) for about 10 h (the necessary pretreatment time before XRD study) after deposition, i.e., after aging for about 30 h. A strong peak located at $2\theta = 64.45°$ can be assigned to the (220) planes of FCC-Ag (JCPDF 89-3722). Two weak peaks located at $2\theta = 35.94°$ and $2\theta = 76.12°$ can be assigned to (10$\bar{1}$0) and (11$\bar{2}$4) or (20$\bar{2}$0) planes of 4H-Ag (JCPDF 87-0598), respectively. This result indicates that 4H-Ag phase exists in GS-Ag sample aging for 30 h but has a low concentration. Figure 3b shows the XRD pattern of the same sample after aging at room temperature for about 4 months; the reflection of 4H phase increases dramatically, indicating that the phase transition from FCC-Ag phase to 4H-Ag phase could happen even at room temperature. This structure transition could also happen more quickly when the GS-Ag sample was heated at higher temperature, for example, at 90 °C in our experiments. Recently, Zhu et al.[26] reported that 4H-Ag nanowires can coexist with FCC-Ag nanowires prepared by electrochemical deposition, and their calculation showed that the 4H-Ag phase is energetically favorable in the diameter ranging from 10 to 50 nm. Our TEM observations also show that dense stacking faults in the

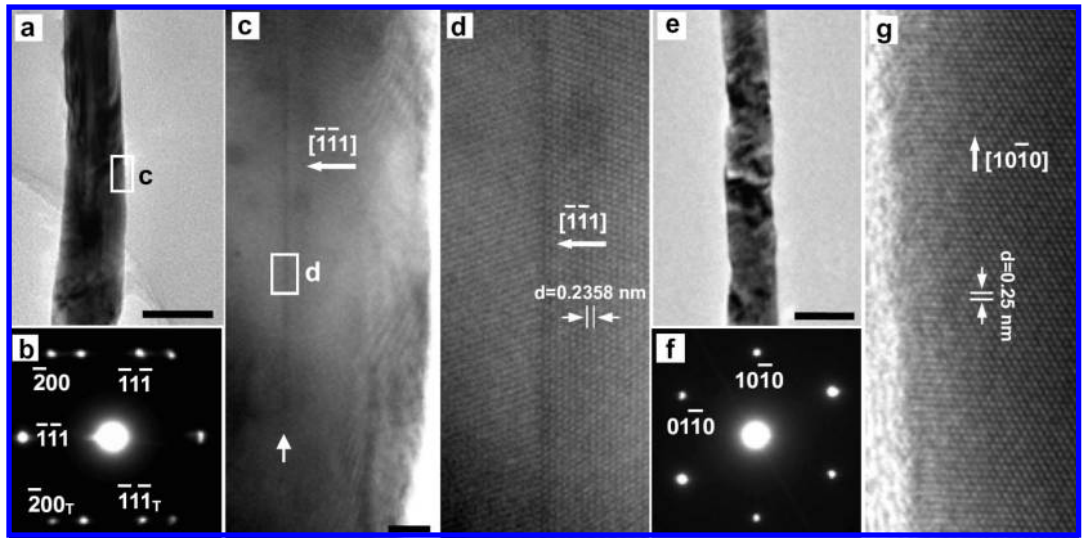

Figure 4. Ag nanowires selected from GS-Ag nanowires sample after heating: (a) TEM image of a single-crystal FCC-Ag nanowire, whose longitudinal axis is [110], scale bar 50 nm; (b) an electron diffraction pattern from this nanowire indexed as FCC-Ag; (c) HRTEM image of the boxed area in (a) of this FCC-Ag nanowire at low magnification, only one growth twin (indexed by arrowhead) parallel to the wire axis exists in this area, scale bar 5 nm; (d) HRTEM image of FCC-Ag nanowire at high magnification, a growth twin exists in the center of this image; (e) TEM image of a single-crystal 4H−Ag nanowire, scale bar 50 nm; (f) an electron diffraction pattern from this nanowire indexed as 4H-Ag; (g) HRTEM image of the 4H-Ag nanowire.

Ag nanowires disappear, and both 4H-Ag and FCC-Ag nanowires could be found in the samples after aging or heating. Figure 4a,e shows that FCC-Ag and 4H−Ag nanowires grow along [110] and [10$\bar{1}$0] directions, respectively. This sample was heated at 90 °C for 2 h before the TEM observation. The corresponding electron diffraction patterns (Figure 4b,f) and HRTEM images (Figure 4c,d,g) are shown next to each TEM image. From the diffraction patterns and HRTEM we know that the stacking faults all disappeared, while few growth twins still existed in the single-crystal FCC-Ag nanowires after heating, which indicates that the phase transition from GS-Ag nanowires to the single-crystal 4H−Ag or FCC-Ag nanowires could happen in the heating process.

It is well-known that the FCC-Ag structure can be represented in terms of the stacking of its close-packed (111) planes with the sequence ABCABC... while the 4H packing (ABCBABCB.... type packing) can be considered as an example of the stacking faults for the FCC crystals.[27] Since the 4H structure is energetically favorable for the nanowire with the diameter around 40 nm and dense (111) stacking faults exist in as-prepared GS-Ag nanowires,[26] it is reasonable that the phase transition from GS-Ag nanowires into 4H-Ag nanowires would occur in heat treatment. It is well-known that there is a plane relation between hexagonal and cubic structure: $(0001)_h$ // $(111)_c$. From the HRTEM image in Figure 2, we found that the (111) plane of GS-Ag nanowires is parallel to the wire long axis. So the (0001) plane of 4H-Ag nanowires, which comes from the (111) plane of GS-Ag nanowire, would be parallel to the nanowire long axis after phase transition. Thus the obtained 4H-Ag nanowires could have a preferred orientation along the [10$\bar{1}$0] direction, which is confirmed by our XRD observation shown in Figure 3. Here our experiments may provide an explanation of why the 4H-Ag phase could form with template method.

GS-Ag nanowires with less planar defects could also change into single-crystal FCC-Ag nanowires in the annealing process when the planar defects just disappear without phase transition. This is proven by our XRD and TEM observations in Figures 3 and 4, respectively.

4. Conclusions

In this study, we developed a two-step electrodeposition method to synthesize large-scale Ag nanowires with dense lengthwise (111) stacking faults and (111)/[112] growth twins. Novel 4H-Ag nanowires with a preferred orientation along the [1010] direction formed spontaneously after aging or heating these GS-Ag nanowires. More generally, oriented attachment and the following dense packing defects formation is not constrained to occur in the electrodeposition process of Ag nanowires;the only requirement is that the deposited metal or alloy has small stacking fault energy. The two-step electrodeposition method used in our experiments may be used to produce different kinds of nanowires with dense stacking faults and growth twins parallel to the nanowire axis. These nanowires could have novel physical properties such as the plasticity, the strength, and the electrical conductivity. This study contributes to the understanding of planar defect formation in electrodeposition and could be used to control the crystallinity of the metallic nanowires.

Acknowledgment. This work was supported by the National Natural Science Foundation of China (Nos. 50671099, 50172048, 10374090 and 10274085), Ministry of Science and Technology of China (No. 2005CB623603), Hundred Talent Program of Chinese Academy of Sciences, and Ningbo Natural Science Foundation (2006A610062).

Supporting Information Available: The illustration of electrochemical cells, the SEM image of empty AAM template and Ag nanowires embedded in AAM, the TEM image of GS-Ag nanowires with diameter of 25 nm, the XRD pattern of common FCC-Ag nanowires sample grown along the [220] direction. This information is available free of charge via the Internet at http: //pubs.acs.org.

References

(1) Favier, F.; Walter, E. C.; Zach, M. P.; Benter, T.; Penner, R. M. *Science* **2001**, *293*, 2227.
(2) Cui, Y.; Wei, Q. Q.; Park, H. Q.; Lieber, C. M. *Science* **2001**, *293*, 1289.
(3) Yi, G.; Schwarzacher, W. *Appl. Phys. Lett.* **1999**, *74*, 1746.
(4) Bietsch, A.; Michel, B. *Appl. Phys. Lett.* **2002**, *80*, 3346.
(5) Lu, L.; Shen, Y. F.; Chen, X. H.; Qian, L. H.; Lu, K. *Science* **2004**, *304*, 422.
(6) Wang, J. G.; Tian, M. L.; Mallouk, T. E.; Chan, M. H. W. *J. Phys. Chem. B* **2004**, *108*, 841.
(7) Merz, M. D.; Dahlgren, S. D. *J. Appl. Phys.* **1975**, *46*, 3235.
(8) Sun, Y. G.; Yin, Y. D.; Mayers, B. T.; Herricks, T.; Xia, Y. N. *Chem. Mater.* **2002**, *14*, 4736.
(9) Terabe, K.; Hasegawa, T.; Nakayama, T.; Aono, M. *Nature* **2005**, *433*, 47.
(10) Jin, R. C.; Cao, Y. W.; Mirkin, C. A.; Kelly, K. L.; Schatz, G. C.; Zheng, J. G. *Science* **2001**, *294*, 1901.
(11) Gould, I. R.; Lenhard, J. R.; Muenter, A. A.; Godleski, S. A.; Farid, S. *J. Am. Chem. Soc.* **2000**, *122*, 11934.
(12) Martin, C. R. *Sciene* **1994**, *266*, 1961.
(13) Choi, J. R.; Oh, S. J.; Ju, H.; Cheon, J. *Nano Lett.* **2005**, *5*, 2179.
(14) Xue, F. H.; Fei, G. T.; Wu, B.; Cui, P.; Zhang, L. D. *J. Am. Chem. Soc.* **2005**, *127*, 15348.
(15) Tian, M. L.; Wang, J. G.; Kurtz, J.; Mallouk, T. E.; Chan, M. H. W. *Nano Lett.* **2003**, *3*, 919.
(16) Zhang, S. H.; Jiang, Z. Y.; Xie, Z. X.; Xu, X.; Huang, R. B.; Zheng, L. S. *J. Phys. Chem. B* **2005**, *109*, 9416.
(17) Uchihashi, T.; Ohbuchi, C.; Tsukamoto, S.; Nakayama1, T. *Phys. Rev. Lett.* **2006**, *96*, 136104.
(18) Switzer, J. A.; Kothari, H. M.; Bohannan, E. W. *J. Phys. Chem. B* **2002**, *106*, 4037.
(19) Masuda, H.; Fukuda, K. *Science* **1995**, *268*, 1466.
(20) Li, A. P.; Müller, F.; Birner, A.; Nielsch, K.; Gösele, U. *J. Appl. Phys.* **1998**, *84*, 6023.
(21) Jessensky, O.; Müller, F.; Gösele, U. *Appl. Phys. Lett.* **1998**, *72*, 1173.
(22) Pan, H.; Sun, H.; Poh, C.; Feng, Y. P.; Lin, J. Y. *Nanotechnology* **2005**, *16*, 1559.
(23) Mehl, M. J.; Papaconstantopoulos, D. A.; Kioussis, N.; Herbranson, M. *Phys. Rev. B* **2000**, *61*, 4894.
(24) Meyer, R.; Lewis, L. J. *Phys. Rev. B* **2002**, *66*, 052106.
(25) Lee, B. J.; Shim, J. H.; Baskes, M. I. *Phys. Rev. B* **2003**, *68*, 144112.
(26) Liu, X. H.; Luo, J.; Zhu, J. *Nano Lett* **2006**, *6*, 408.
(27) Taneja, P.; Banerjee, R.; Ayyub, P. *Phys. Rev. B* **2001**, *64*, 033405.

CG800212Z